Computers in Physics

Chaotic Scattering

Tolga Yalçinkaya and Ying-Cheng Lai

Citation: Computers in Physics **9**, 511 (1995); doi: 10.1063/1.168549
View online: http://dx.doi.org/10.1063/1.168549
View Table of Contents: http://scitation.aip.org/content/aip/journal/cip/9/5?ver=pdfcov
Published by the AIP Publishing

CHAOTIC SCATTERING

Tolga Yalçinkaya and Ying-Cheng Lai

Department Editors: Harvey Gould
hgould@clarku.edu
Jan Tobochnik
jant@kzoo.edu

Scattering is a fundamental tool for studying many physical systems. In a scattering experiment, particles with different initial states interact with the system of interest and the characteristics of the particles after the scattering are recorded. We usually plot an output variable characterizing the particles after the scattering versus an input variable characterizing the particles before the scattering. The relation between the two variables is called the scattering function. It may happen that there is an infinite number of singularities in the scattering function. Near these singularities, arbitrarily small changes in the input variable can cause large changes in the output variable. This sensitive dependence on initial conditions signifies the appearance of chaos.[1]

To illustrate how chaotic scattering arises, we consider a model system proposed by Gaspard and Rice.[2] The system consists of point particles incident on three circular hard disks in a two-dimensional plane, as shown in Fig. 1. We choose the radii of the disks to be $R_1=R_2=R_3=1$. The distances between the individual disks are all $d=2.5$. The disks are located at $x=-d\sqrt{3}/6$, $y=d/2$ (disk 1), $x=d\sqrt{3}/3$, $y=0$ (disk 2), and $x=-d\sqrt{3}/6$, $y=-d/2$ (disk 3). Because the potential function is infinite for regions inside the hard disks and zero outside the disks, a classical particle bounces off a disk when it collides with it. At each collision the angle of incidence equals the angle of reflection (see Fig. 1). A particle coming from $x=-\infty$ spends a finite amount of time in the region between the disks (the scattering region), and then exits to infinity with an angle θ, where θ is defined counterclockwise with respect to the x axis as shown in Figs. 2 and 3. For convenience, we assume that the incident particle trajectory is parallel to the x axis with an impact parameter b, the y distance between the initial particle trajectory and the x axis. The angle with which the particle exits the scattering region depends on the value of the impact parameter, and we write $\theta=\theta(b)$.

Tolga Yalçinkaya is a graduate student in the Department of Physics and Astronomy, The University of Kansas, Lawrence, KS 66045; tolga@poincare.math.ukans.edu. Ying-Cheng Lai is an assistant professor in the Departments of Physics and Astronomy and Mathematics, The University of Kansas, Lawrence, KS 66045; lai@poincare.math.ukans.edu

The time $T(b)$ (the delay time) that the particle spends in the scattering region before exiting also depends on b. Figure 2 shows two particle trajectories with impact parameters $b_1=0.21005$ and $b_2=0.21010$, respectively. The corresponding scattering angles and delay times are $\theta(b_1)\approx 5.63511$ and $\theta(b_2)\approx 5.63168$, and $T(b_1)\approx 21.745$ and $T(b_2)\approx 21.743$. The delay time is defined as the time during which the particles remain within a distance $R=10$ ($R\gg R_i,d;i=1, 2, 3$) from the origin. The initial particle velocities are assumed to be unity. In this case $|b_1-b_2|=5\times10^{-4}$, $|\theta(b_1)-\theta(b_2)|\approx 0.003$, and $|T(b_1)-T(b_2)|\approx 0.002$. That is, a small difference in the impact parameter b leads to small differences in the scattering angles and the delay times, a situation that we would typically expect. This behavior implies that the scattering function $\theta(b)$ and the delay time function $T(b)$ near b_1 and b_2 are smooth functions of b.

More complicated dynamics can occur as seen in Fig. 3, where two particle trajectories with impact parameters $b_1=0.33005$ and $b_2=0.33010$ are shown. The difference $|b_2-b_1|=5\times10^{-4}$ is the same as in the first case. The scattering angles for these two trajectories are $\theta(b_1)\approx 3.717$ and

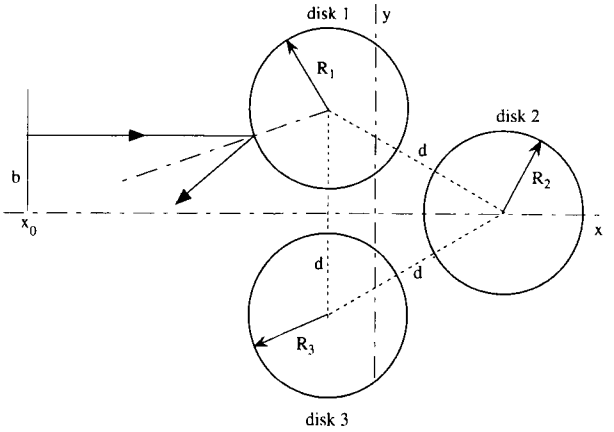

Figure 1. The Gaspard–Rice scattering system. The radii of the three hard disks are $R_1=R_2=R_3$, and the distances between the disks are all $d=2.5$.

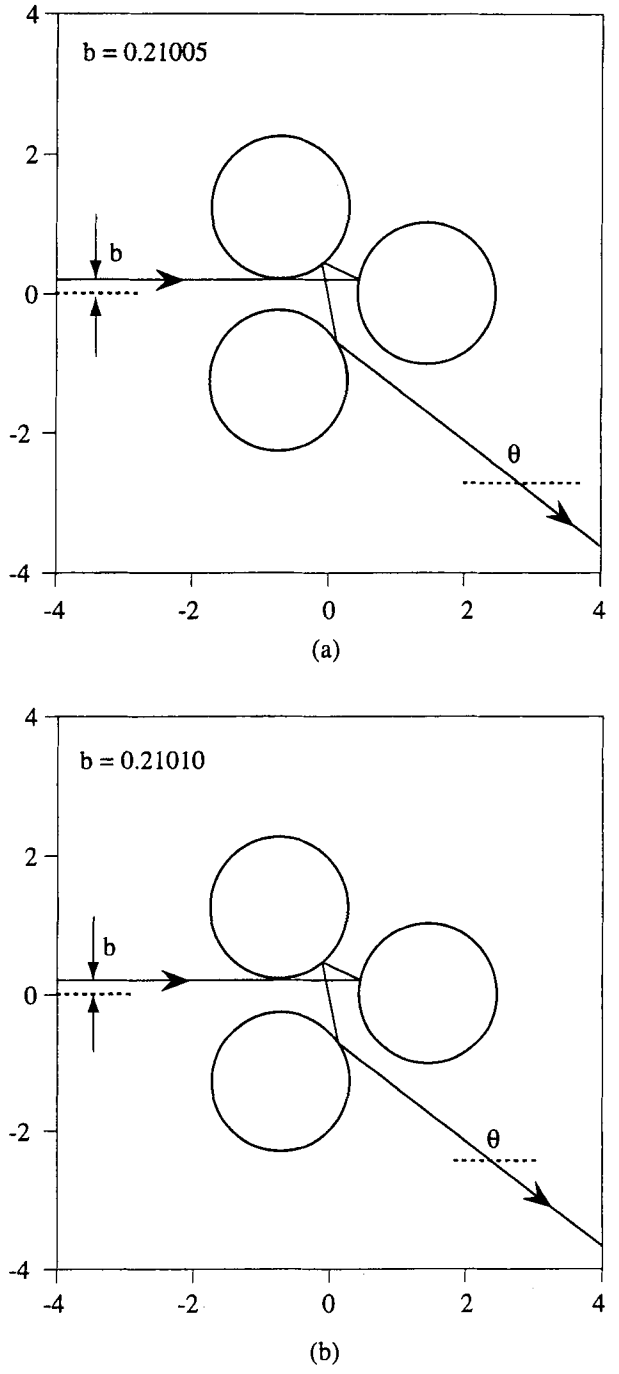

Figure 2. Two particle trajectories with impact parameters b_1=0.21005 and b_2=0.21010, respectively.

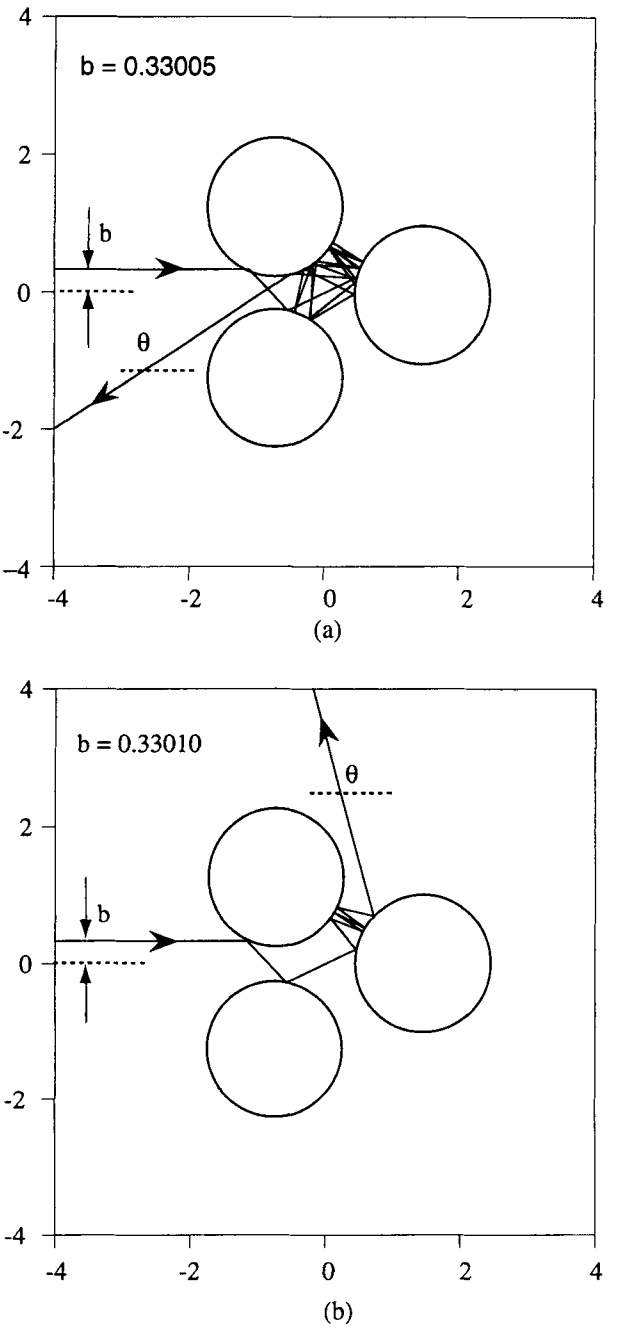

Figure 3. Two particle trajectories with impact parameters b_1=0.33005 and b_2=0.33010, respectively.

$\theta(b_2)\approx 1.879$, and the difference is $\Delta\theta=|\theta(b_2)-\theta(b_1)|=1.878$, which is the order of 2π, the maximum possible difference in the scattering angles. Such a large difference in the scattering angles is reflected in the large difference in the delay times, because particle 1 experiences substantially more bounces in the region between the three disks than particle 2 does despite the very small difference in their impact parameters (see Fig. 3). The delay times are $T(b_1)\approx 33.271$ and $T(b_2)\approx 23.471$, and the difference $\Delta T=|T(b_2)-T(b_1)|=9.8$, which is more than four orders of magnitude larger than the difference in the impact parameters. Hence, around the impact parameters $b\approx 0.33$, a small difference in the initial condition leads to a big difference in the outcome of the trajectories. This sensitive

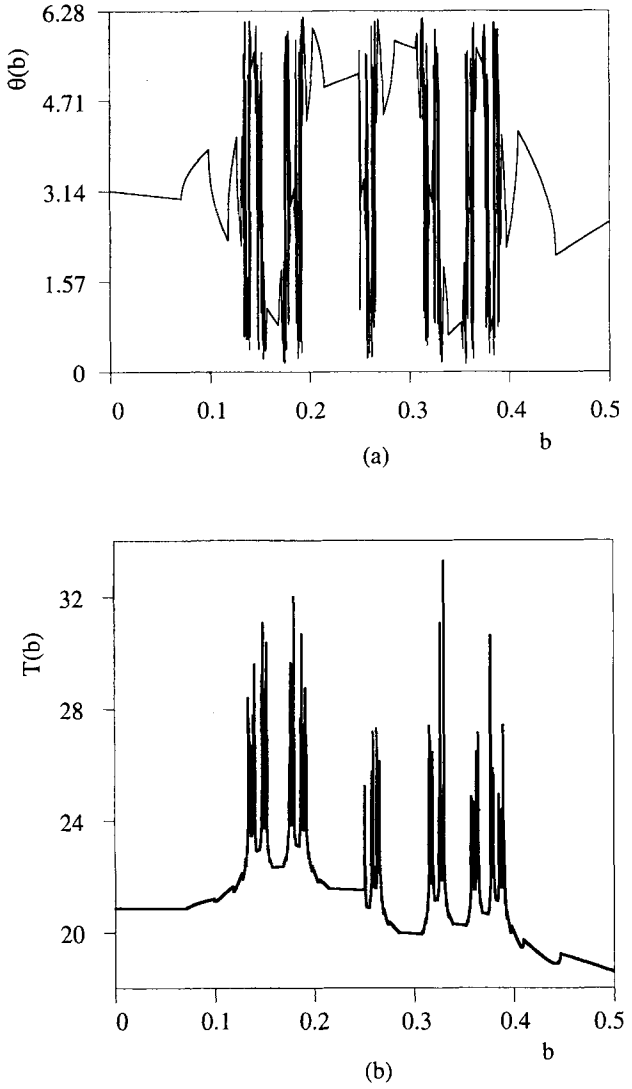

Figure 4. The scattering function (a) and the delay time function (b) for $0 \leq b \leq 0.5$.

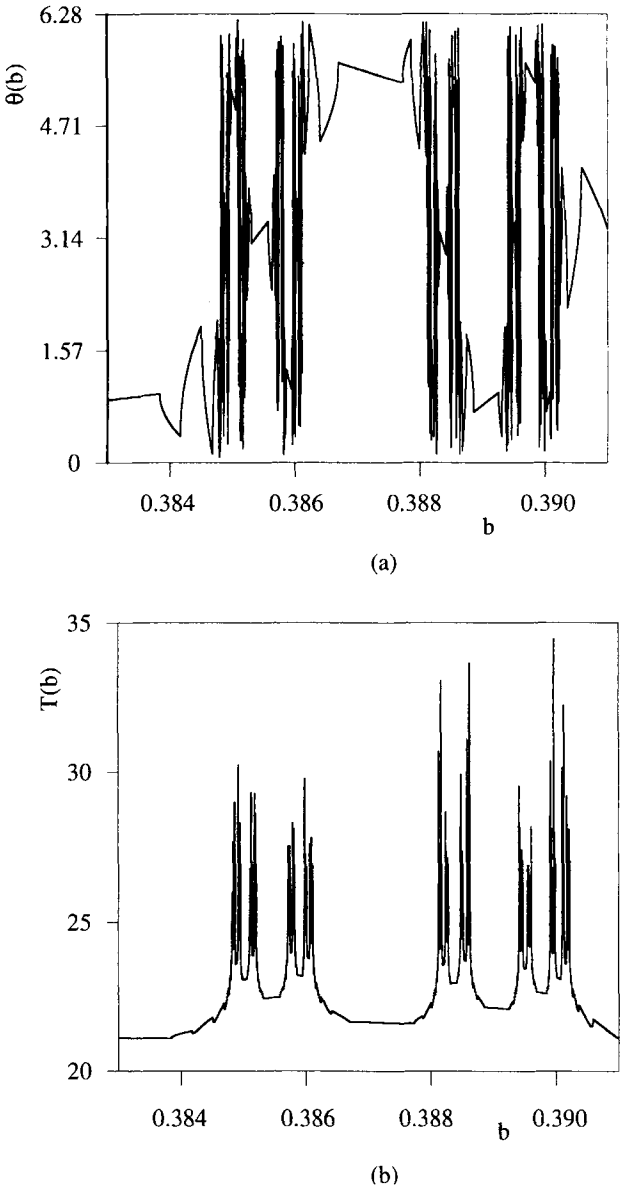

Figure 5. Blowups of the scattering function (a) and the delay time function (b) for $0.383 \leq b \leq 0.391$.

dependence on initial condition is a clear signature of chaos.

Although Fig. 3 is for one pair of impact parameters, the sensitive dependence on initial conditions commonly occurs at many impact parameters (in fact, an infinite number of them). This behavior can be seen in Fig. 4 where $\theta(b)$ and $T(b)$ are plotted for 10^4 values of b in the range $0 \leq b \leq 0.5$. It is apparent that these plots contain both smooth and wildly oscillating parts, the dynamics of which correspond to Figs. 2 and 3, respectively. The mixture of smooth and wildly oscillating behavior in $\theta(b)$ and $T(b)$ repeats itself on smaller scales. Figure 5 shows that the behavior of $\theta(b)$ and $T(b)$ for $0.383 \leq b \leq 0.391$ is similar to the behavior shown in Fig. 4. Further blowups of Fig. 5 would reveal similar features. The repetition of certain dynamical features at different scales is typical of fractal sets. In fact, there exists a fractal set of an infinite number of b values at which $\theta(b)$ and $T(b)$ have singularities. This dependence on b is typical of chaotic scattering.

To further quantify the nature of chaotic scattering, it is convenient to compute the fractal dimension for the set of singularities in the scattering and delay time functions. The dimension of a set can be defined by the box-counting dimension (capacity).[3] To compute this fractal dimension, we cover the set with a grid of boxes of side length ϵ. Let $N(\epsilon)$ be the number of boxes needed to cover the whole set. Then $N(\epsilon)$ increases as ϵ decreases, and typically scales as

$N(\epsilon) \sim \epsilon^{-D_0}$, where D_0 is the box-counting dimension of the set. More rigorously, we have,

$$D_0 = \lim_{\epsilon \to 0} \frac{\ln N(\epsilon)}{\ln(1/\epsilon)}. \quad (1)$$

It can be easily verified that Eq. (1) yields the correct dimension for conventional sets such as a line segment and a finite area in the plane.[4] To compute the value of D_0 for the set of singularities in the scattering function, we simply count the boxes needed to cover the singularities at different scales ϵ. The slope of the fitted line on the plot of $\ln N(\epsilon)$ versus $\ln(1/\epsilon)$ is an estimate of the value of D_0. To obtain a robust fitting, it is necessary to vary ϵ over several orders of magnitude. Such a task is usually difficult, if not impossible, because $N(\epsilon)$ greatly increases as ϵ decreases, and we seek alternative methods to compute the fractal dimension.

A more convenient fractal dimension to compute, which is often used to characterize chaotic scattering, is the uncertainty dimension.[5–8] The uncertainty dimension was first introduced by Grebógi *et al.*[9] to characterize fractal basin boundaries, which arise commonly in dissipative chaotic systems with multiple attractors.[9,10] It has been conjectured that the uncertainty dimension is equal to the box-counting dimension for typical chaotic sets.[11,12] The procedure for computing the uncertainty dimension is as follows. For an arbitrary location on the left of the scattering region ($x_0 = -10$ in our example), we randomly choose an impact parameter b as in Fig. 1. We then make a small perturbation to this initial condition to obtain a nearby initial condition $b+\epsilon$. The scattering trajectories of particles originating from these two initial conditions are computed. If the number of bounces in the scattering region experienced by the two particles is the same, we call the first initial condition to be "certain" against small perturbations. This behavior occurs if the initial condition is chosen to be in the range where the scattering and delay time functions are smooth (see Figs. 4 and 5). However, due to the presence of singularities in these functions, it may happen that the two nearby initial conditions will lead to trajectories that behave very differently. In particular, the number of bounces in between the hard disks will differ. We call such initial conditions "uncertain" against small perturbations. For a given perturbation ϵ, we can compute the fraction of uncertain initial conditions $f(\epsilon)$ for many randomly chosen initial conditions. In our numerical experiments, $f(\epsilon)$ is obtained by accumulating 200 uncertain initial conditions among N total initial conditions, that is, $f(\epsilon) = 200/N$. As ϵ decreases, we expect $f(\epsilon)$ to decrease as well. In most physical situations, $f(\epsilon)$ scales with ϵ as

$$f(\epsilon) \sim \epsilon^{\alpha}, \quad (2)$$

where α is the uncertainty exponent.[9,10] The dimension of the fractal set is given by $D = 1 - \alpha$. Intuitively, obtaining the number of uncertain initial conditions for perturbations of different orders of magnitude is equivalent to counting the number of singularities in the scattering and delay time functions for different scales. Hence, we expect that the uncertainty dimension is a good approximation to the box-counting dimension. The uncertainty algorithm offers a great computational advantage because it requires relatively little memory in comparison to the box-counting procedure whose memory requirements become severe since the number of boxes required to cover the set increases as a power law as we go to smaller scales.

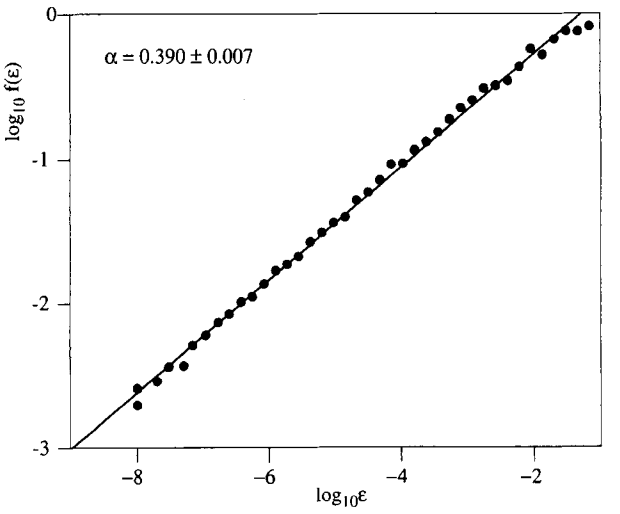

Figure 6. The uncertain fraction $f(\epsilon)$ vs the perturbation ϵ on a logarithmic scale. The uncertainty exponent is $\alpha = 0.390 \pm 0.007$. The fractal dimension of the set of singularities in the scattering and delay-time functions is $d = 1 - \alpha = 0.610 \pm 0.007$.

Figure 6 shows the uncertainty fraction $f(\epsilon)$ versus the perturbation ϵ on a logarithmic scale, where ϵ varies by seven orders of magnitude. The plot can be robustly fitted by a straight line, the slope of which is $\alpha = 0.390 \pm 0.007$. We conclude that the fractal dimension of the set of singularities in the scattering and delay-time functions is $D = 1 - \alpha = 0.610 \pm 0.007$.

The dynamical mechanism for the occurrence of chaotic scattering is the existence of an invariant set that contains an *infinite number of unstable periodic orbits* in the scattering region. By periodic orbits we mean those particle trajectories that repeat themselves after a certain number of bounces in between the hard disks. Consequently, these trajectories are trapped in the scattering region forever. Figure 7 shows some examples of such periodic orbits, with three period-two orbits (orbits that repeat themselves after two bounces) and a period-three orbit (an orbit that repeats itself after three bounces). These periodic orbits are unstable. That is, perturbations to the orbit, no matter how small, will result in deviation away from the periodic orbit and lead to an exit of the particle out of the scattering region. For the Gaspard–Rice three disk system, periodic orbits can be conveniently represented by abstract symbols.[2] Suppose that we label a particle trajectory by

$$a_1 a_2 a_3 \cdots a_{n-1} a_n a_{n+1} \cdots , \quad (3)$$

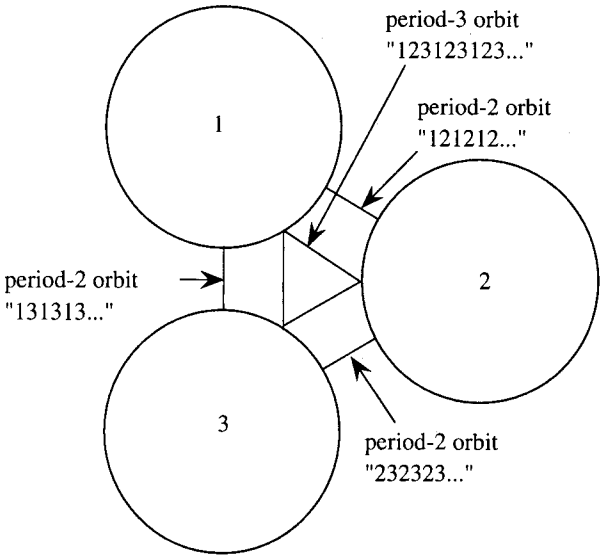

Figure 7. Three unstable period-two orbits, one unstable period-three orbit, and their symbolic representations.

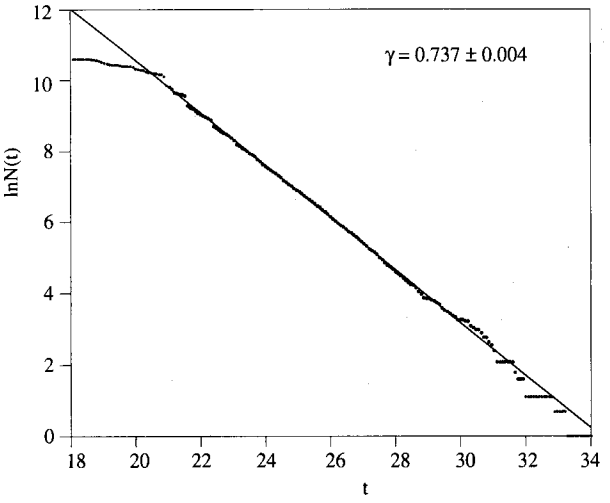

Figure 8. Exponential decay of particle trajectories from the scattering region.

where $a_n = i$ if the trajectory bounces off disk i at the nth bounce. Because a typical scattering trajectory eventually exits the scattering region, the corresponding symbol representation Eq. (3) only has a finite number of symbols. Periodic orbits are represented by a string of infinite symbols which consists of the repetition of a certain finite number of symbols. For example, the three period-two orbits in Fig. 7 can be represented by 121212..., 232323..., and 131313..., respectively, and the period-3 orbit can be represented by 123123123... (or 231231231... and 312312312...). As the period p of the orbit increases, the number of orbits increases exponentially, because the number of ways of representing a string of the length $p(a_1 a_2 \cdots a_{p-1} a_p)$ increases exponentially as a function of p. This simple argument implies that there must be an infinite number of periodic orbits for the Gaspard–Rice scattering system. Moreover, all periodic orbits are unstable. Besides these periodic orbits, there are also trajectories that wander in the scattering region forever but never repeat themselves, as can be seen again via the symbol representation shown in Eq. (3). There are also an infinite number of aperiodic trajectories (also termed chaotic trajectories). These aperiodic trajectories, together with the infinite number of unstable periodic orbits, make up a chaotic invariant set in the scattering region. This set is invariant in the sense that trajectories in the set stay in the set forever. The most important feature about this chaotic set is that it is *nonattracting*. That is, trajectories starting from randomly chosen initial conditions may wander near the chaotic set for a finite amount of time before exiting. In mathematical terms, the chaotic invariant set has a Lebesgue measure zero,[4] meaning that the probability for trajectories originating from random initial conditions to land precisely on the chaotic set is zero.

Although the chaotic invariant set has a Lebesgue measure zero, its existence renders chaotic the scattering dynamics. A typical trajectory will wander in the vicinity of the chaotic set for a while before exiting. Due to the chaotic nature of the invariant set, another trajectory starting from a slightly different initial condition may wander in the vicinity of the chaotic set for a drastically different amount of time before exiting. This behavior gives rise to the sensitive dependence on initial conditions and, consequently, to the set of an infinite number of singularities in the scattering and delay-time functions.

The existence of the nonattracting chaotic invariant set in the scattering region can be detected by monitoring how particles decay from the scattering region. We can launch many particles with different impact parameters towards the scattering region and examine the number of particles left in the region as time progresses. If there is a nonattracting chaotic set, the number of particles remaining in the scattering region at time t, denoted by $N(t)$, decays exponentially,

$$N(t) \sim \exp(-\gamma t), \tag{4}$$

where γ is the decay rate.[13] The decay is exponential because of the unstable nature of the periodic and aperiodic orbits in the chaotic set. Such a chaotic set is also said to be "hyperbolic." Figure 8 shows the decay on a semilogarithmic plot for 4×10^4 particles with impact parameters uniformly distributed in the interval [0, 0.5]. A particle is counted as having left the scattering region if it is traveling away from the center of the scattering region (the origin of the $x-y$ coordinate in Fig. 1) beyond $R = 10$. Initially, $N(t)$ deviates somewhat from the exponential law, because most of the particles have not entered the scattering region by $t \approx 21$. The exponential decay starts at $t \approx 21$, by which time most particles are already in the scattering region wander-

ing in the vicinity of the chaotic set and are starting to escape. The data for $21 \leq t \leq 31$ can be fitted by a straight line, indicating exponential decay. For $t > 31$, the data again deviates from the straight line fit. This deviation is due to the lack of sufficient statistics because there are only about 10 particles left at $t = 31$. The overall behavior of Fig. 8 strongly suggests that the decay of particles is exponential, a signature of a chaotic invariant set in the scattering region.[13]

The above exploration of the Gaspard–Rice scattering system establishes that chaotic scattering is due to the existence of nonattracting chaotic invariant sets in phase space that contain an infinite number of unstable periodic orbits and aperiodic orbits. The chaotic invariant set is responsible for the set of singularities in the scattering and delay-time functions. Chaotic scattering occurs commonly in real physical systems. In the past decade, chaotic scattering has been found by workers in many disciplines including astrophysics,[14] fluid mechanics,[15] chemistry,[16] and solid-state physics.[17] Chaotic scattering also may occur in time-dependent Hamiltonian systems.[6]

An interesting question that has been explored during the past few years is how chaotic scattering arises as a system parameter changes (bifurcation to chaotic scattering). Various studies have revealed that there are two basic routes to chaotic scattering. The first is the so-called "abrupt" bifurcation in which a chaotic invariant set is suddenly created as a system parameter changes through a critical value.[13] The abrupt bifurcation to chaotic scattering was investigated by Bleher, Grebogi, and Ott.[13] They illustrated this phenomenon for a two-dimensional potential of the form $V(x,y) = x^2 y^2 e^{-(x^2+y^2)}$. This potential has four peaks at $x,y = \pm 1$, with the height of each peak being $V_m = 1/e^2$. The potential rapidly drops to zero in regions away from the origin. Particles coming toward the potential from far away will spend some time in the region where the potential is appreciable and then exit to infinity. If the particle energy E is larger than V_m, the particle can penetrate each of the four potential peaks and escape. In this case, the scattering is not chaotic. As soon as the $E < V_m$, particles can no longer penetrate the potential peaks and will bounce back and forth between the four potential peaks, a situation similar to the Gaspard–Rice system. In this case, the scattering is chaotic. If we regard the particle energy as a control parameter, then as E is decreased through V_m, a chaotic invariant set is suddenly created, giving rise to an abrupt bifurcation to chaotic scattering. We briefly mention that the second route to chaotic scattering is similar to the period-doubling bifurcation to chaos in dissipative dynamical systems.[18] This route to chaotic scattering can be seen[19] in a system of three "soft" circular potential peaks arranged as in Fig. 1, where "soft" means that the potential function has finite values so that particles can enter the potential region and have their trajectories bent inside the disks.

In terms of the dynamical properties of the chaotic invariant set, the dynamics of chaotic scattering may be characterized as either *hyperbolic*[13] or *nonhyperbolic*[5,19,20] In hyperbolic chaotic scattering, all the periodic orbits are unstable, and the survival probability $P(t)$ of a particle in the scattering region decays exponentially, as in the Gaspard–Rice system. A situation can occur where particles originating from certain regions of a *nonzero area* can be trapped inside the scattering region forever. In this case, the trapped region is stable [the region is defined by the Kolmogorov–Arnold–Moser (KAM) surfaces]. Chaotic invariant sets exist outside the KAM surfaces. Chaotic scattering is nonhyperbolic in this case. A distinct feature of nonhyperbolic chaotic scattering is that particles initially in a region that contains the chaotic invariant sets can spend a long time in the vicinity of KAM surfaces. This scattering leads to algebraic decay of the survival probability of the particles:

$$P(t) \sim t^{-z}, \quad (t \gg 1), \tag{5}$$

where z is the algebraic decay exponent. This behavior is in contrast to the exponential decay in the hyperbolic case. Algebraic decay is a common feature of chaotic systems that contain KAM surfaces.[21–23]

After the onset of chaotic scattering, qualitative changes in the characteristics of the scattering can occur as the control parameter is varied further. One recent result in hyperbolic chaotic scattering is the so-called "crisis in chaotic scattering"[7,8] for which two preexisting, topologically and dynamically isolated chaotic invariant sets in phase space collide with each other to form a single chaotic set. Consequently, an uncountably infinite number of new periodic and chaotic trajectories is suddenly created once the crisis occurs, and the fractal dimension of the set of singularities in the scattering function increases during the crisis, giving rise to an enhancement of chaotic scattering. For nonhyperbolic chaotic scattering, recent numerical investigations have revealed that the algebraic decay exponent z may exhibit rather large changes as a control parameter is varied. These changes can be attributed to the continual process of the breakup of KAM surfaces in phase space.[20] This result has potential relevance to the microwave ionization of Rydberg hydrogen atoms.[24] In this case, published studies indicate that, contrary to naive physical intuition, the ionization rate, analogous to the decay exponent z in our case, is not a monotonically increasing function of the field strength, and in many instances an increase of the field strength actually leads to a decline of the ionization rate.[24]

An important direction of research in chaotic scattering is the study of the quantum mechanics of systems that exhibit chaotic scattering in the classical limit. Such a study is particularly relevant to problems such as ballistic electron transport in mesoscopic junction systems in solid state physics.[17] Studies of the quantum manifestation of chaotic scattering[17,25,26] show that the elements of the scattering matrix (S matrix) exhibit rapidly varying changes in their dependence on the energy. The origin of these quantum fluctuations is the occurrence of chaotic scattering when the system is treated classically. An interesting recent study showed that the rapidly varying changes in the matrix elements of $S(E)$ are characteristically greatly enhanced in the nonhyperbolic case in comparison to the hyperbolic case.[26] We mention that the general problem of quantum chaos,

which refers to the study of the quantum properties of systems whose classical physics is chaotic, is a very active field of research.

In conclusion, we have introduced the phenomenon of chaotic scattering using a simple model system. We also have discussed the physical mechanism and dynamical origin of the occurrence of chaotic scattering. The key result is that chaotic scattering is due to a nonattracting chaotic invariant set that contains an infinite number of unstable periodic and aperiodic orbits. We also briefly discussed advanced topics such as hyperbolic and nonhyperbolic chaotic scattering and quantum manifestations of chaotic scattering.

Suggestions for further work

Writing a program to simulate the Gaspard–Rice scattering system is difficult because it is nontrivial to monitor a trajectory that bounces back and forth in between the hard disks. A good understanding of chaotic scattering can be obtained by considering a simpler model based on a discrete map. The map is two dimensional and is given by[5]

$$x_{n+1}=f(x_n,y_n)\equiv a(x_n-\tfrac{1}{4}(x_n+y_n)^2),$$
$$y_{n+1}=g(x_n,y_n)\equiv\frac{1}{a}(y_n+\tfrac{1}{4}(x_n+y_n)^2), \tag{6}$$

where x and y are the dynamical variables of the map, and $a>1$ is a control parameter of the system. For large values of x and y, the quadratic terms in Eq. (6) dominate, and x quickly moves to $-\infty$. In this sense, the map models a situation that is similar to scattering. In addition, it is easy to see that any initial condition for which $x<0$ maps to $x=-\infty$. Thus, any invariant set of Eq. (6) must satisfy $x\geq 0$.

(1) To become familiar with the map Eq. (6), first find the fixed points of the map defined by $f(x,y)=x$ and $g(x,y)=y$. There are two fixed points of the map. Examine the stability of these fixed points. Show that one fixed point is always unstable, and the other is stable for $1<a<a_0$ and unstable for $a\geq a_0$. Find the value of a_0.

(2) Fix the parameter a at $a=8.0$. Choose initial conditions on the horizontal line defined by $y_0=-0.3$. Choose 10^4 initial conditions with x_0 uniformly distributed in the range $0\leq x_0\leq 0.1$, and compute the delay time function $T(x_0)$. For a given value of x_0, T is defined as the number of iterations it takes for the trajectory to reach $x=-5.0$. (For $x<-5$, the trajectory quickly diverges to $x=-\infty$.) If there is a value of x_0 such that $T(x_0)>7$, then choose 10^4 new initial conditions centered about this value of x_0 on a smaller interval. Repeat this process as many times as you can, and convince yourself that large values of $T(x_0)$ occur at arbitrarily small scales of x_0.

(3) Apply the uncertainty algorithm to compute the fractal dimension of the set of singularities in the delay time function $T(x_0)$. Determine $f(\epsilon)$ for $\epsilon=10^{-p}$ and $p=2$ to 8. An initial condition x_0 is counted as uncertain if the delay time of the trajectories changes when x_0 is changed to $x_0+\epsilon$. Plot $\ln f(\epsilon)$ versus $\ln \epsilon$. Fit the data with a straight line, the slope of which is the uncertainty exponent α.

(4) Choose 4×10^4 initial conditions with $y_0=-0.3$ and the values of x_0 uniformly distributed in the interval $0\leq x_0\leq 0.1$. A trajectory is considered to have escaped the scattering region if $x<-5$. Compute the maximum escape time $t_{\max}$ among these 4×10^4 particles. Compute the number of particles $N(t)$ still left in the scattering region as a function of time t for $0<t<t_{\max}$. Plot $\ln N(t)$ against t. Is the decay exponential? If yes, what is the exponential decay rate? (The scattering in this case is hyperbolic.)

(5) Change the parameter to $a=4.1$. Take 100 initial conditions uniformly distributed in the two-dimensional region $1.00<x_0\leq 1.05$ and $0.60\leq y_0\leq 0.65$ and plot 10^3 iterations for each initial condition. If a trajectory escapes, plot the trajectory before $x_n<-5$. What do you observe? You will find that for some initial conditions, the trajectory will trace out a closed curve. Regions enclosed by such closed curves correspond to initial conditions that never escape the scattering region (KAM surfaces). This example is a case of nonhyperbolic chaotic scattering.

(6) Choose many initial conditions in a region that appears to not contain any KAM surfaces and compute $N(t)$. To find such a region, refer to Eq. (5) to get an idea of the approximate locations of the KAM surfaces. Then choose a small region that apparently does not contain any KAM surfaces. You will find that the decay is no longer exponential, but is algebraic. Plot $\ln N(t)$ versus $\ln t$, and compute the algebraic decay exponent. Note that, because KAM surfaces exist on arbitrarily small scales, it is likely that the region from which initial conditions are chosen contains some very small KAM surfaces. As a consequence, you may find a few particles that never decay and, hence, $N(t)$ will not be zero even if t is very large. However, this behavior does not affect the calculation of $N(t)$, and we can subtract from $N(t)$ the small number of particles in the KAM surfaces that are still trapped for t very large.

Acknowledgments

The authors wish to thank the editors, Harvey Gould and Jan Tobochnik, for their helpful comments and suggestions. This work was supported by the Kansas Institute for Theoretical and Computational Science through the NSF/K*STAR Program.

From the editors. Remember that the success of this column depends on your input. Please send us your results, comments, and suggestions for future columns. The second edition of our computer simulation text has now been published by Addison-Wesley and a World Wide Web server has been established as a forum for users of our text and faculty and students using computer simulations in an educational context.

References

1. *Focus Issue on Chaotic Scattering,* T. Tél and E. Ott, editors, Chaos **3**, 417 (1993).
2. P. Gaspard and S. A. Rice, J. Chem. Phys. **90**, 2225 (1989).
3. J. D. Farmer, E. Ott, and J. A. Yorke, Physica D **7**, 153 (1983).
4. E. Ott, *Chaos in Dynamical Systems* (Cambridge University Press, New York, 1993).
5. Y. T. Lau, J. M. Finn, and E. Ott, Phys. Rev. Lett. **66**, 978 (1991).
6. Y. C. Lai and C. Grebogi, Int. J. Bif. Chaos **1**, 667 (1991).
7. Y. C. Lai, C. Grebogi, R. Blümel, and I. Kan, Phys. Rev. Lett. **71**, 2212 (1993).
8. Y. C. Lai and C. Grebogi, Phys. Rev. E **49**, 3761 (1994).
9. C. Grebogi, S. W. McDonald, E. Ott, and J. A. Yorke, Phys. Lett. A **99**, 415 (1983).
10. S. W. McDonald, C. Grebogi, E. Ott, and J. A. Yorke, Physica D **17**, 125 (1985).
11. C. Grebogi, H. E. Nusse, E. Ott, and J. A. Yorke, in *Dynamical Systems,* edited by J. C. Alexander, Lecture Notes in Mathematics Vol. 1342 (Springer, Berlin, 1988), p. 220.
12. H. E. Nusse and J. A. Yorke, Commun. Math. Phys. **150**, 1 (1992).
13. S. Bleher, C. Grebogi, and E. Ott, Physica D **46**, 87 (1990).
14. P. T. Boyd and S. L. W. McMillian, Chaos **4**, 507 (1993).
15. C. Jung, E. Tél, and E. M. Ziemniak, Chaos **3**, 555 (1993).
16. D. W. Noid, S. Gray, and S. A. Rice, J. Chem. Phys. **85**, 2649 (1986).
17. R. A. Jalabert, H. U. Baranger, and A. D. Stone, Phys. Rev. Lett. **65**, 2442 (1990).
18. M. J. Feigenbaum, Los Alamos Sci. **1**, 4 (1980).
19. M. Ding, C. Grebogi, E. Ott, and J. A. Yorke, Phys. Rev. A **42**, 7025 (1990).
20. Y. C. Lai, M. Ding, C. Grebogi, and R. Blümel, Phys. Rev. A **46**, 4661 (1992).
21. C. F. F. Karney, Physica D **8**, 360 (1983).
22. B. V. Chirikov and D. L. Shepelkyansky, Physica D **13**, 395 (1984).
23. J. D. Meiss and E. Ott, Phys. Rev. Lett. **55**, 2741 (1985).
24. Y. C. Lai, C. Grebogi, R. Blümel, and M. Ding, Phys. Rev. A **45**, 8284 (1992).
25. R. Blümel and U. Smilansky, Phys. Rev. Lett. **60**, 477 (1988).
26. Y. C. Lai, R. Blümel, E. Ott, and C. Grebogi, Phys. Rev. Lett. **68**, 3491 (1992).